

Macroscopic Quantum Interference Effects through Superconducting Point Contacts

J. E. ZIMMERMAN AND A. H. SILVER

Scientific Laboratory, Ford Motor Company, Dearborn, Michigan

(Received 9 August 1965)

A small-area contact between two pieces of superconducting metal or alloy is a remarkably sensitive and convenient device for demonstrating long-range quantum interference effects. It has been shown in many experiments that the critical supercurrent through a pair of such contacts in a parallel superconducting circuit has a component periodic in the flux enclosed by the topological ring formed by the parallel circuit, the periodicity being $h/2e$, showing that the wave function is coherent around the ring. With this configuration we have demonstrated coherence lengths of the order of millimeters or centimeters in Nb, V, Ta, Sn, Pb, and $\text{Nb}_{0.85}\text{Zr}_{0.15}$, in rings where the enclosed area was as large as 1 cm^2 , so that the periodicity in applied field was of the order of 10^{-7} G . Both bulk and thin-film materials have been used. These experiments provide general proof of London's concept of long-range phase coherence in both type-I and type-II superconductors, and in addition lead to useful laboratory instruments. We have used such devices to show quantized flux pinning in bulk type-II superconductors and to measure the magnetic field of a rotating superconductor.

I. INTRODUCTION

THE term "quantum interference" or "interference effect" has recently been used to describe a number of experiments with weakly coupled superconductors and superconducting rings, in which the experimental results are interpretable quite directly in terms of London's concept of a wave function coherent over the entire superconductor. These experiments are in some cases closely analogous to diffraction and interference effects of ordinary electromagnetic waves.

The flux quantization experiments of Deaver and Fairbank,¹ and Doll and Nabauer² were the first demonstrations of macroscopic quantization in a superconductor, and a convincing confirmation of London's insight³ into the fundamental significance of the superconducting state. The later theoretical predictions that the fundamental particle of superconductivity is the electron pair and that the flux quantum is of magnitude $h/2e$ rather than h/e as London originally guessed were also confirmed.

Following the theoretical paper by Josephson⁴ on superconducting tunneling through thin insulating barriers, there has arisen a class of experiments which, in addition to providing beautiful demonstrations of the wave nature of electrons, flux quantization, etc., on a macroscopic scale, also show promise of leading to a variety of useful laboratory techniques and instruments. Josephson predicted a dc supercurrent through the (rectangular) barrier of the form

$$j = j_0 \sin\left(\Delta\gamma - \frac{2e}{\hbar} \int A dl\right), \quad (1)$$

where $\Delta\gamma - (2e/\hbar) \int A dl$ is the phase shift across the

junction. From this the total current across the junction in the presence of an applied magnetic field is

$$I = I_0 \frac{|\sin(\varphi_j e/\hbar)|}{\varphi_j e/\hbar}, \quad (2)$$

where φ_j is the flux in the junction produced by a field parallel to an edge, and I_0 is the maximum supercurrent of the junction. This expression is formally identical to that for Fraunhofer diffraction. Josephson's predictions of both dc and ac supercurrents were shortly put to test and were verified by Anderson and Rowell,⁵ Shapiro,⁶ and others.^{7,8}

The preceding experiments were carried out on a comparatively small scale. Experiments by Jaklevic, Lambe, Silver, and Mercereau⁹ on a pair of Josephson junctions in parallel and by Lambe, Silver, Mercereau, and Jaklevic¹⁰ on thin-film rings interrupted by a pair of narrow constrictions (bridges), produced results on a truly macroscopic scale, of the order of millimeters. It was in connection with the Jaklevic experiments that the term "interference effect" came to be used, the experiments being interpreted in terms of coherent interference of the wave function over the two parallel paths provided by the experimental topology (ring). Thus, for two identical oxide barriers in parallel, the total current, assuming no field on the barriers themselves, is

$$I = I_1 + I_2 = I_0(\sin\gamma_1 + \sin\gamma_2), \quad (3)$$

where γ_1 and γ_2 are the phase shifts across the two junctions, respectively. In order that the wave function be

⁵ P. W. Anderson and J. M. Rowell, *Phys. Rev. Letters* **10**, 230 (1963).

⁶ S. Shapiro, *Phys. Rev. Letters* **11**, 80 (1963).

⁷ M. D. Fiske, *Rev. Mod. Phys.* **36**, 221 (1963).

⁸ J. M. Rowell, *Phys. Rev. Letters* **11**, 200 (1963).

⁹ R. C. Jaklevic, J. Lambe, A. H. Silver, and J. E. Mercereau, *Phys. Rev. Letters* **12**, 503 (1964); **12**, 514 (1964); R. C. Jaklevic *et al.*, in Ninth International Conference on Low Temperature Physics (to be published).

¹⁰ J. Lambe, A. H. Silver, J. E. Mercereau, and R. C. Jaklevic, *Phys. Letters* **11**, 15 (1964).

¹ B. S. Deaver and W. M. Fairbank, *Phys. Rev. Letters* **7**, 43 (1961).

² R. Doll and M. Nabauer, *Phys. Rev. Letters* **7**, 51 (1961).

³ F. London, *Superfluids* (Dover Publications Inc., New York, 1960), Vol. I.

⁴ B. D. Josephson, *Phys. Letters* **1**, 251 (1962); *Rev. Mod. Phys.* **36**, 216 (1964).

single-valued, these must satisfy the condition

$$\gamma_1 - \gamma_2 + \oint \frac{2e}{\hbar} \mathbf{A} \cdot d\mathbf{l} = 2\pi n, \quad n=0, \pm 1, \pm 2, \dots, \quad (4)$$

where the integral of vector potential A around the ring is equal to the enclosed flux φ_{int} . Taking $n=0$, it follows from straightforward manipulation that

$$I = 2I_0 \cos((e/\hbar) \varphi_{\text{int}}) \sin(\gamma_A - \gamma_B), \quad (5)$$

where γ_A and γ_B are the relative phases at two arbitrary reference points on opposite sides of the ring. Critical current I_c corresponds to $\gamma_A - \gamma_B$ being $\pm \frac{1}{2}\pi$, thus,

$$I_c = 2I_0 |\cos((e/\hbar) \varphi_{\text{int}})| \quad (6)$$

and the periodicity in flux is $h/2e$, not h/e as might appear at first glance. This equation predicts the peak-to-peak amplitude ΔI_c of the interference pattern to be $2I_0$, i.e., I_c should vary between zero and $2I_0$ with varying field. In general this is not what was observed experimentally. Experimentally it was found that ΔI_c was often considerably smaller than $2I_0$, and simple arguments suggest that ΔI_c may be equal to $2I_0$ or to φ_0/L , whichever is smaller, where L is the inductance of the ring. The simplest way to interpret this result is to recall that φ_0/L is the value of circulating current necessary to contain one flux quantum within the ring.

The experiments discussed in the preceding paragraph tend to direct attention away from the weak links (bridges or oxide barriers) and toward the properties of the ring as a whole and the flux through it; the weak link becomes a device, like the slit of an interferometer, for localizing and controlling the phase of the wave function so as ultimately to produce an interference pattern. We wish to emphasize that the periodicity, and indeed the existence, of the interference pattern comes as a consequence of Eq. (4); only the detailed shape of the pattern comes from the actual functional dependence of j on γ , as for example that given by Eq. (1). The point is that, although one may use Josephson's equation as a starting point in a calculation, this is not rigorous for metal bridges or point contacts; other assumptions regarding the relationship between current and phase shift lead to qualitatively similar results.

The work described in this paper was inspired by the need for a simple experimental technique applicable to all superconductors. There are many questions, obvious and otherwise, which one might hope to answer thereby: for example, whether long-range phase coherence is a property of all superconductors, type I and type II; what is the maximum area and/or perimeter of rings in which flux quantization is observable; what is the maximum amplitude of the interference effect, and others. There are a number of difficulties attending the use of thin films and oxide barriers for interference experiments. It is difficult to produce thin films of many pure metals, to say nothing of alloys, and most experi-

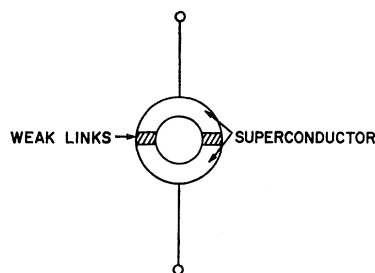


FIG. 1. Topology of the interference effect. The weak links may be oxide barriers, point contacts, or narrow constrictions in the ring.

ments have been done on tin and lead; relatively few on other metals. The oxide barrier, usually formed by oxidation of the base metal, must be exceedingly thin, of the order of 10 or 20 Å, and generally seems to lack reproducibility and long-term stability. It may be argued that the observation of persistent currents in superconducting magnets shows that the range of phase coherence is at least of the order of miles. But this merely repeats London's argument; the observation of flux quantization is something more. It is intriguing, to say the least, to think of demonstrating flux quantization in a system in the, say, 10^{13} excited state. Present technique is probably not adequate to do this; however, it is conceivable that one might be able to show whether the field of a persistent current magnet at the 100 kG level varies by as much as 10^{-8} G.

The fundamental topology of these interference experiments is a superconducting ring interrupted by a pair of weak links as shown in Fig. 1. The weak links may be thin oxide barriers, narrow metallic bridges or small area contacts (probably a variation of the metallic bridge). This paper deals with the last case specifically. Two terminals are indicated in Fig. 1 for connection to associated circuitry. For dc and low-frequency work we frequently use four terminals (separate current and potential leads). In their microwave experiments Lambe, Silver, Mercereau, and Jaklevic¹⁰ used capacitive coupling to the ring with no direct connections at all. It has also been shown that at high frequencies only one weak link in the ring is required.¹¹ Here we talk about only the dc and low-frequency characteristics of devices of the type shown in Fig. 1, in which the weak links are small area or "point" contacts

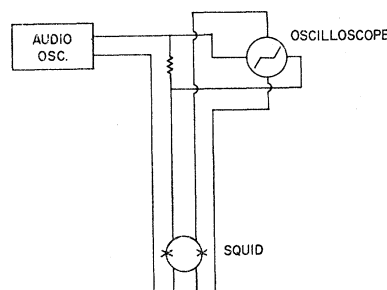


FIG. 2. Circuit used for displaying the volt-ampere characteristics of point contacts. SQUID is an abbreviation of superconducting quantum interference device.

¹¹ A. H. Silver, J. E. Mercereau, and J. E. Zimmerman, *Bull. Am. Phys. Soc. Ser. II*, **10**, 318 (1965). A. H. Silver and J. E. Zimmerman (to be published).

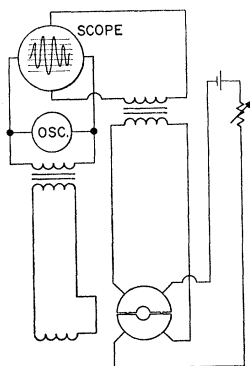
between the two sections of the ring. The analogy between these quantum-mechanical interference experiments and the double-slit interference of light is useful because it leads immediately to the idea of more complicated topologies than that of Fig. 1, and in the extreme case to the magnetic analog of the diffraction grating. A simple experiment with a multiple-contact device will be described. All measurements, except where otherwise specified, were made at about 4.2°K.

II. EXPERIMENTAL METHODS AND RESULTS

A. The Interference Effect

Our initial experiments with macroscopically single-point contacts have been briefly described in the literature.¹² These experiments were carried out with small-diameter wires, or wire and ribbon, connected in the circuit of Fig. 2 for observing volt-ampere characteristics, and in the circuit of Fig. 3 for observing interference patterns. In the latter circuit, the horizontal oscilloscope sweep was usually linear in time, and was synchronized with the sinusoidal oscillator voltage. Hence most of the interference patterns shown in what follows appear as frequency-modulated wave trains. A synchronous detector and x - y recorder could be added to the latter circuit for recording interference patterns, though usually it was more convenient to photograph the oscilloscope trace. The wires were held mutually perpendicular in a simple micarta jig, with a force of a few grams on the contact point. Some selected results are shown in Figs. 4(a) and 4(b). Many of the patterns obtained with crossed wires were much more complicated than this. In extreme cases the pattern seemed to be completely irregular, like random noise, and yet was perfectly reproducible provided the contact was not disturbed. We have been able to obtain periodic patterns with every superconductor tried; this includes Nb, V, Ta, Pb, and a Nb-Zr alloy (Fig. 5), and various combinations where the two wires were of different metals (e.g., Ta and Pb). The smallest periodicity in applied field observed for any pair of crossed wires was about 0.1 G, and there was no apparent upper limit.

FIG. 3. Circuit used for observing interference patterns.



¹² J. E. Zimmerman and A. H. Silver, *Phys. Letters* **10**, 47 (1964).

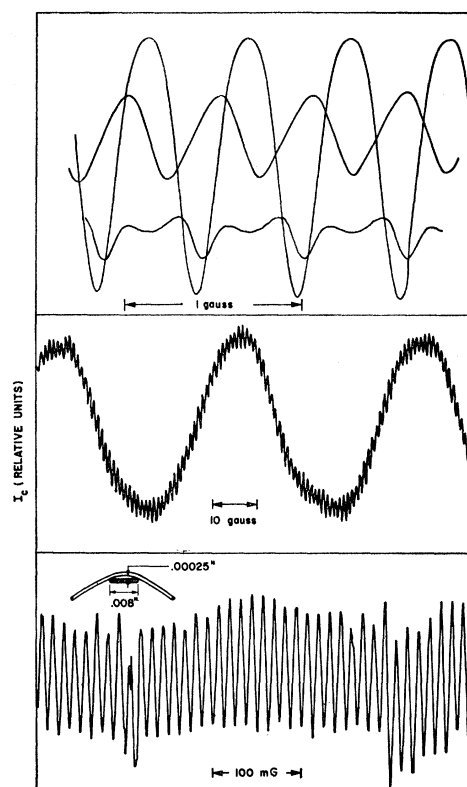


FIG. 4. Interference patterns obtained with niobium point contacts. Upper and middle patterns from crossed wires. Lower pattern from geometry shown in the inset.

Our interpretation of these results, in terms of multiple microscopic contacts due to surface roughness, will be presented in the next section. All of the experiments now to be described utilized two or more macroscopically separate contacts. A contact which would be regarded as "multiple" in the above sense will be regarded as "single" in the context of what follows, where the physical separation of two contacts is large compared to the separation of the surface asperities within the individual contact areas.

Figure 4(c) shows the result obtained with the experimental configuration of a wire bent across a thin ribbon so as to enclose a lens-shaped area of the size shown in the inset. A variation on this arrangement, shown in Fig. 6, consists of a pair of linked "hairpins." With enclosed areas as large as 0.1 mm², this arrangement produced periodicities in field as small as 2×10^{-4} G. Some "devices" of this type, held in fixed configuration by a drop of epoxy cement, showed consistent behavior over a period of weeks. Crossed wire devices of the type described have certain advantages, such as absurd simplicity; however, devices more useful for some purposes have been machined from bar stock. Figure 7(a) shows the cross section of such a device, in which the point contacts were formed by raising a burr or chip of metal with a scalpel on each side of the center

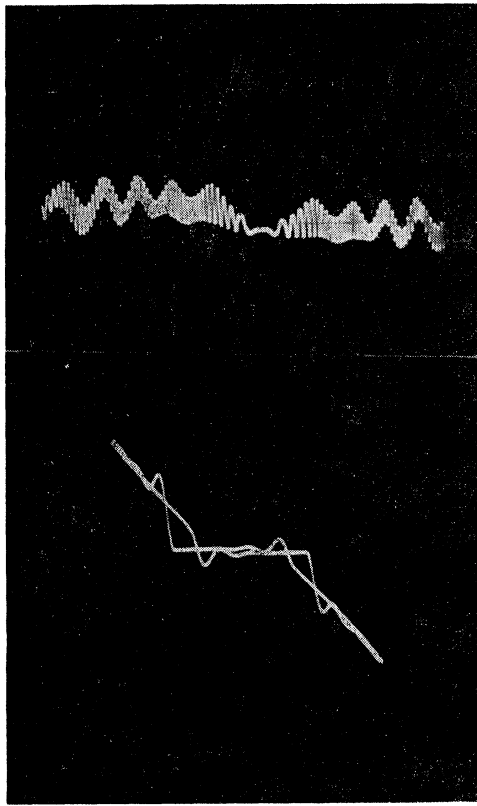


FIG. 5. Volt-ampere characteristic and interference pattern of crossed wires of Nb-Zr (15%) alloy.

hole. The two halves of the device were held together by a nonshorting clamp. Varying the clamping pressure served as a crude adjustment for the point contacts. A device of this type with a center hole 0.003 in. in diameter was used for the observation of individual flux quanta pinned in 0.002-in. Nb wires.¹³

Eventually, however, it became apparent that the above methods of making point contacts were quite unpredictable and what has finally evolved is a refinement of the structure of Fig. 7(b). The refinement consists of superconducting screws (000-120) with lock nuts, set one on each side of the center hole to serve as adjustable

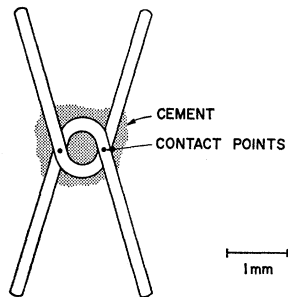


FIG. 6. "Linked-hairpin" type of interference device.

¹³ J. E. Zimmerman and J. E. Mercereau, Phys. Rev. Letters **13**, 125 (1964).

contact points. In addition, a mechanical linkage was designed and built for adjusting the screws while the interference device was in the cryostat and operating. A structure like this, with screw contacts, has been made with a center hole 1 cm in diameter, giving a periodicity of $\sim 2 \times 10^{-7}$ G applied field. Owing to this high sensitivity, it was necessary to use three Mumetal cylinders around the cryostat and a superconducting lead cylinder in the liquid helium, to shield against stray field fluctuations. It was also essential to guard against any vibration of the components relative to each other, and to use heavy rf filtering in all leads going into the cryostat. The interference pattern is shown in Fig. 8. A device like

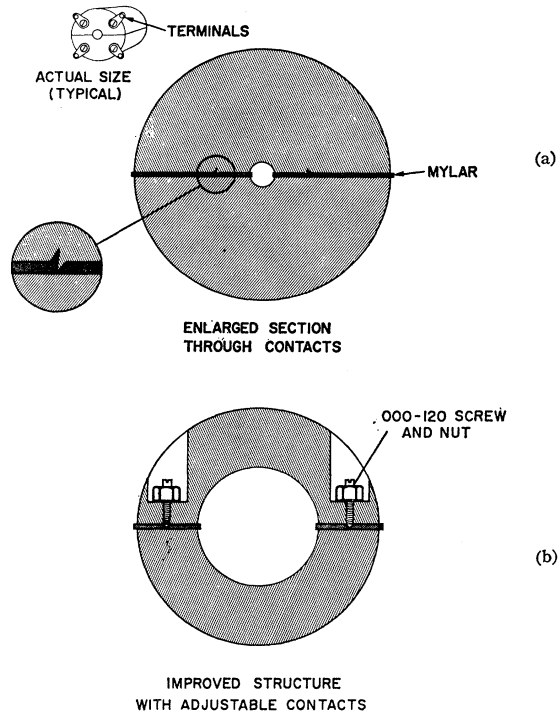


FIG. 7. Constriction of large-area point-contact interference devices. Upper section shows the use of surface flaws or burrs as point contacts. Lower section showing the use of pointed screws is preferable. Screws can be adjusted by rods or other suitable linkage from outside the cryostat.

this was used to measure the magnetic field due to its own rotation at a rate of ~ 1 rotation/sec.¹⁴ The noise appearing on the pattern falls in a frequency band of approximately 50 to 2000 cps. Critical current of the contacts was varied (by adjusting the screws) between a few tenths and a few tens of microamperes without significantly affecting the interference pattern. The amplitude of the upper pattern in Fig. 8 corresponds to $\Delta I_c \sim 0.2 \mu\text{A}$. For comparison, the calculated inductance of the structure was $L \sim 5 \times 10^{-9}$ H, giving $\varphi_0/L \sim 0.4 \mu\text{A}$.

¹⁴ J. E. Zimmerman and J. E. Mercereau, Phys. Rev. Letters (to be published).

Similar qualitative or semiquantitative observations have been made on a number of smaller rings of various shapes. To summarize: (1) the amplitude ΔI_c of the interference pattern is of the order of, or less than, φ_0/L , and is no greater than the sum of the critical currents I_{c1} and I_{c2} of the two contacts taken separately; (2) in cases where the sum of critical currents is less than φ_0/L , ΔI_c may equal $I_{c1} + I_{c2}$, i.e., the interference pattern may modulate between zero and $I_{c1} + I_{c2}$; (3) provided I_{c1} and I_{c2} are each greater than φ_0/L , ΔI_c may approach quite closely the limiting value φ_0/L , even though I_{c1} and I_{c2} may differ by a factor of 100 or so, and (4) for a particular setting of the screws, there may be no interference pattern at all, even though both contacts are apparently superconducting; however, we were able invariably to obtain the interference effect with a minimum of persistence in adjusting the contacts. With regard to the first three of these observations, one would suppose on theoretical grounds that the amplitude ΔI_c of the interference pattern could not be greater than the smaller of I_{c1} or I_{c2} . Therefore, in order that the interference pattern modulate to zero, I_{c1} must equal I_{c2} . This supposition has not been checked experimentally. An example of a volt-ampere characteristic where the critical current modulates nearly to zero is shown in Fig. 9. The photograph shows a superposition of the traces for four different field values. For clarity, the traces for maximum and minimum critical current, respectively, are sketched below the photograph. The data were obtained with a niobium screw-contact type device.

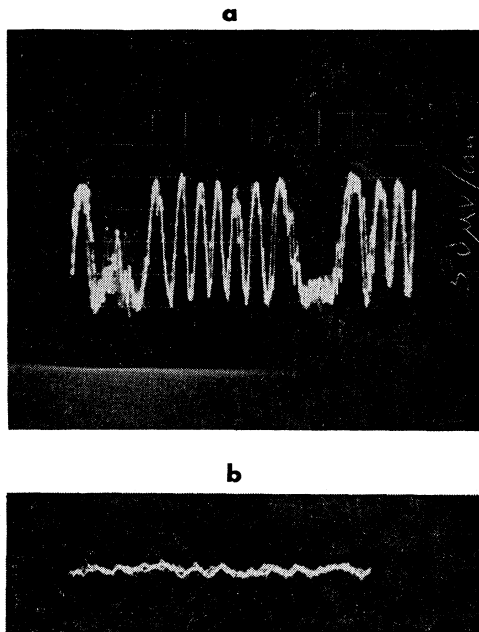


FIG. 8. Interference patterns of large-area devices in which noise is apparent. Both patterns are from devices like that shown in the lower part of Fig. 7. Dimensions: upper trace, $\frac{1}{4}$ in. i.d., $\frac{3}{4}$ in. o.d., $\frac{3}{8}$ in. long; lower trace, $\frac{3}{8}$ in. i.d., $\frac{3}{4}$ in. o.d., $\frac{3}{8}$ in. long. All leads into the cryostat were heavily filtered for frequencies above about 10^6 .

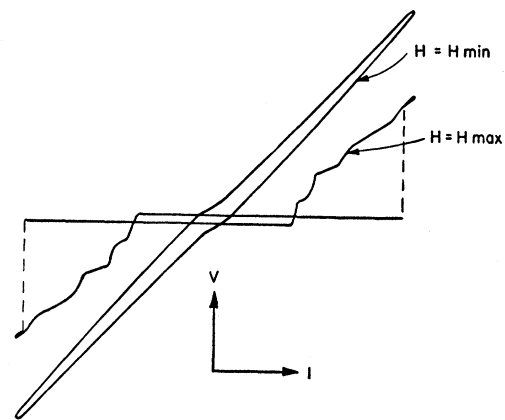
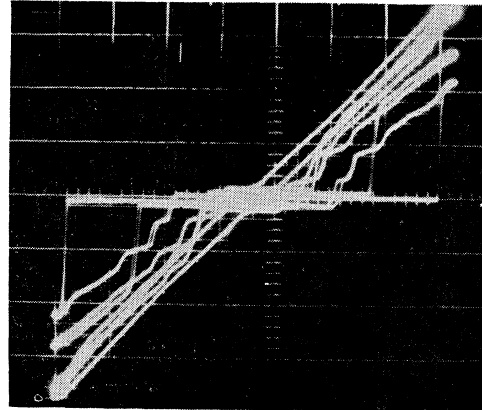


FIG. 9. Magnetic-field modulation of the volt-ampere characteristic for a (nontypical) case where I_c goes to zero periodically. The photograph is a superposition of traces for four different field values. The lower sketch is a tracing, for clarity of the two lines for which I_c is maximum and minimum, respectively.

The above-mentioned 1-cm (internal-diameter) device encloses the largest area in which the interference effect has been observed. Larger area devices seem quite feasible; the limitation would be the increasing sensitivity to noise. The longest *distance* over which the effect was seen was 15 cm. This was with a Sn thin-film device using oxide barriers rather than point contacts, and the enclosed area was about 10^{-8} cm².¹⁵ This and other experiments give no hint of a limiting distance over which phase coherence persists, provided the enclosed area is kept small.

Another thin-film experiment, using vanadium, was carried out as follows: The vanadium thin film on glass was clamped firmly against a flat niobium slab, with a sheet of 0.001-in. Mylar interspersed for insulation. The niobium slab was drilled and tapped for a pair of 000–120 niobium contact screws 4 mm apart. The screws were adjusted, by methods already described, to puncture the Mylar and make contact with the vana-

¹⁵ The thin-film experiments were done in collaboration with Dr. Jaklevic.

dium thin film. External circuit connections to the niobium slab and to the film were made with indium solder at points well removed from the contacts. With a 1300-Å film, the contacts were adjusted for a normal-state resistance at 4.2 deg of 1.5Ω . The critical current modulated between 5.5 and 10 μA with the expected periodicity of about 200 μG . Similar results were achieved also with a 600 Å film.

Figure 10 is a drawing of a six-contact interference device and the associated interference pattern. It was expected that this device should behave qualitatively like a six-slit diffraction grating, and the sharply peaked interference pattern seems to bear this out. Each slot of the device was 0.06 mm^2 in area, and point contacts between slots were made with a scalpel as described above. The observed periodicity was about 600 μG , compared to the expected value of 340. However, the applied field in the experimental setup could not be accurately calculated, and also there was no indication that all of the contacts were operating.

B. Volt-Ampere Characteristics

Volt-ampere characteristics of point contacts are characterized by two parameters, the maximum supercurrent I_c and the normal-state resistance R . We define R as the slope of the V - I characteristic at some point outside the zero-voltage region. This corresponds to a sort of intermediate state in which some small region in the immediate vicinity of the contact is nonsuperconducting owing to the high current density; the bulk of the material remains superconducting. The break from superconductivity to normal conduction may be either continuous or discontinuous as shown by typical results (Fig. 11). As one should expect, there is some sort of rough correlation between R and I_c . This is predictable since both R and I_c for a given material depend only upon the radius of the contact, assuming a round contact between two semi-infinite blocks of metal. Experimentally with Nb-Nb contacts we found that I_c varied from a few milliamperes to less than

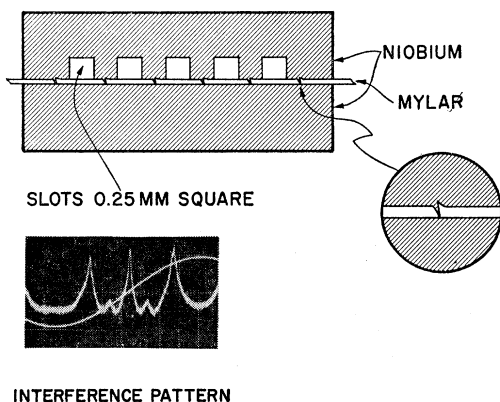


Fig. 10. Cross section of magnetic "diffraction grating" and interference pattern. Peak-to-peak field amplitude 1.8 mG.

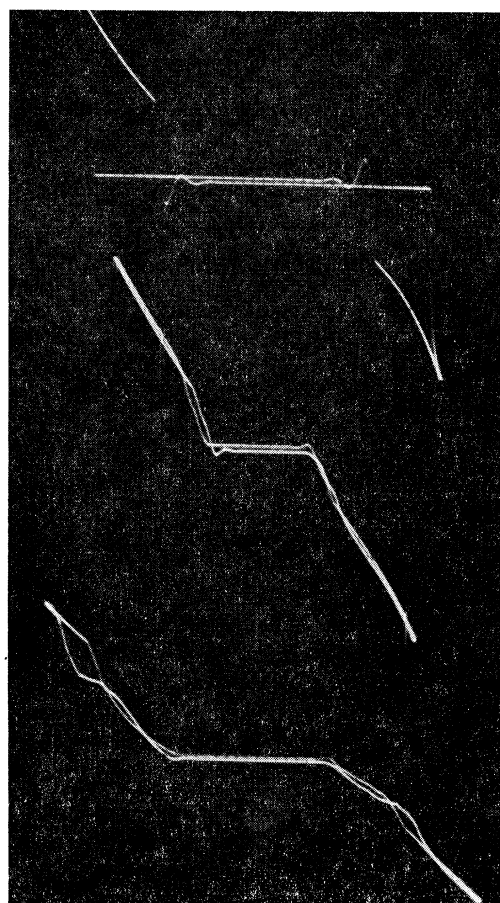


Fig. 11. "Typical" volt-ampere characteristics of point contacts.

10^{-6} A for normal-state resistances from a few tenths to a hundred ohms. The correlation was very rough, and it was soon concluded that the normal-state resistance, either at room or at helium temperature, could not be used to predict I_c . The nature of the relationship between R and I_c is shown by the data in Fig. 12 for three different contacts at 4.2°K. The tantalum used in obtaining the single data point shown had been deoxidized by heating in a high vacuum, hence the relatively low contact resistance. A similar test with deoxidized niobium also resulted in low contact resistance and a critical current beyond the range of the apparatus.

Figures 5, 9, and 11 demonstrate that the V - I characteristics of point contacts can be quite complicated, with kinks and hysteresis loops in the limbs as well as at I_c . This is probably related to the microstructure of the contact itself, but the details of the relationship are not understood. Possibly the most interesting point is that interference effects, if any, are usually observable at these secondary kinks and loops as well as at I_c . This clearly indicates that phase coherence through the contact is maintained even though the contact is not superconducting in the ordinary sense. Phenomena like this have been studied

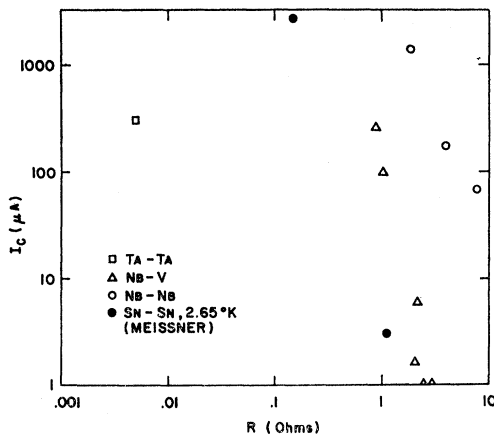


FIG. 12. Plot of low-temperature normal-state resistance (see text) versus critical current for various point contacts.

experimentally and theoretically by Anderson *et al.*,^{16,17} but it does not seem possible to interpret our effects quantitatively.

C. Further Instrumentation

It is apparent that the nature of the interference effect which we have described for a multiply connected superconductor has numerous device implications. We present here one mode of operation which we have accomplished. The circuit of Fig. 3 is extended as shown in the block diagram of Fig. 13. The current bias is adjusted so that the maximum signal amplitude interference pattern is observed as the magnetic field is swept. At this value of bias current, the field sweep is reduced so that the total scan of the interference pattern is approximately $\varphi_0/2L$. The output of the phase detector as a function of applied field is essentially the derivative of the interference voltage signal as shown in Figs. 4 or 8. At the integral flux values this curve has a discriminator-like characteristic and the addition of the operational amplifier, integrator, and field control coil results in "locking" the device to the local extremum value of the interference pattern. Variations in the

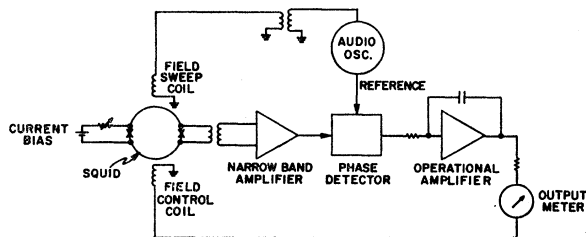


FIG. 13. Block diagram of servo-system used for magnetometry and related applications.

¹⁶ P. W. Anderson and A. H. Dayem, Phys. Rev. Letters 13, 195 (1964).

¹⁷ P. W. Anderson, N. R. Wertheimer, and J. M. Luttinger, Phys. Rev. 138, A1157 (1965).

ambient flux, by whatever mechanism, are observed as a change in the control current; hence the control current is a direct measure of magnetic flux and field. Using a 167 cps audiofrequency and about 0.1-sec response time, we have successfully locked the most sensitive device discussed above, namely one with a field period of 2×10^{-7} G. By this method we have detected field changes of less than 10^{-2} of the field period, or about 10^{-9} G.

The greatest sensitivity is clearly achieved when the flux measured is less than $(h/2e)$. For greater values one might take advantage of the obvious digital nature of the system. Hence we have simultaneously an analog and a digital device which may be of great technological importance.

III. DISCUSSION OF RESULTS

Qualitative interpretation of the interference effects follows quite directly from the Introduction. The first results with single contacts [Figs. 4(a) and 4(b)] are explained on the reasonable assumption that the "contact" in fact consists of a multiplicity of microscopic or

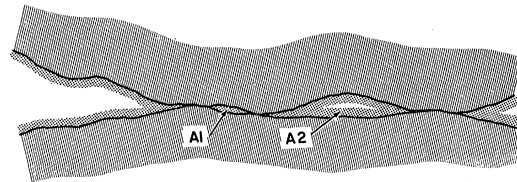


FIG. 14. Model of "point contact" used in interpreting results of Figs. 4 and 5.

submicroscopic areas of actual metallic contact. The critical current would then exhibit a periodicity in field corresponding to the area enclosed between any pair of such actual contacts. Figure 14 illustrates this model for the case of three actual contacts, with two enclosed areas A_1 and A_2 . Such a model might be used in interpreting the pattern of Fig. 4(b). The 1 G periodicity would require an enclosed area of about 2×10^{-7} cm². Assuming the enclosed area to lie mostly within the penetration-depth region of the metal rather than in free space, and taking the penetration depth $\sim 10^{-5}$ cm, gives the distance between contacts $\sim 10^{-3}$ cm or less, depending upon an estimate of demagnetizing factors. This is not unreasonable for wires 0.013 cm in diameter, however, we should not expect periodicities smaller than ~ 1 G for perpendicularly crossed wires, and this is in agreement with experiment. Since the "enclosed area" includes a penetration-depth band within the metal, the periodicity in field should vary with temperature as the penetration depth varies with temperature. This effect has recently been used as the basis of a method of measuring variations of the penetration depth with temperature.¹⁸

¹⁸ R. Meservey, Bull. Am. Phys. Soc. Ser. II 10, 317 (1965).

Comparison between these experiments and those of Little and Parks¹⁹ suggests a unified interpretation in which the two experiments represent opposite extremes of the same basic phenomenon. It is clear that the interpretation of both experiments involves the concept of phase coherence over macroscopic distances. Little and Parks measured the axial resistance of hollow thin-film cylinders at the transition temperature, and found that this varied periodically with applied field. The essential experimental technique was to operate at a precisely controlled temperature within the superconducting-to-normal transition region, thus permitting flux to enter the cylinder while at the same time maintaining phase coherence around the circumference. In our experiments the ring is at all times well below the transition temperature, and flux is permitted to enter through the point contact, which is operated in the region of critical current. Our measurement consists of the observation of the V - I characteristic as a function of field. Since the V - I characteristic is highly nonlinear, it is not appropriate to call this a resistance measurement.

Meyers and Little²⁰ extended these measurements to several type-II superconductors, and were able to show quantum effects in all but vanadium. Since we have here shown interference phenomena in vanadium rings several millimeters in diameter and also in thin films, it appears that the negative result of Meyers and Little is not of fundamental significance. It is conceivable, since in their experiments the measuring current and the circulating currents are orthogonal, that in a slightly inhomogeneous film phase coherence around the cylinder might be lost before a measurable resistance appears in the axial direction. It is difficult to see, however, why such an effect could manifest itself only in vanadium.

We wish now to speculate on the nature of the point contact, on the basis of our meager experimental evidence, namely the contact resistance, contact pressure, critical supercurrent, and so forth. Two obvious models suggest themselves: (1) that an insulating surface film (oxides, etc.) on the metal provides a tunneling barrier of the Josephson type, and (2) that the contact pressure ruptures the surface film and makes metal-to-metal contact. Let us assume the second model, and further assume that the metal in the region of the contact has the properties of the bulk metal. Then we can calculate the effective contact radius r from the contact resistance R , namely $r = \frac{1}{2}\rho/R$, where ρ is the resistivity of the metal. Taking $\rho \sim 10^{-6} \Omega \text{ cm}$, and $R \sim 10 \Omega$ gives $r \sim 10^{-7} \text{ cm}$, only 10 \AA . Another clue to the contact area is provided by the critical supercurrent I_c . Assuming a critical density of 10^6 A/cm^2 , and $I_c \sim 10^{-6} \text{ A}$ gives a contact area of 10^{-12} cm^2 , or a radius of $\sim 10^{-6} \text{ cm}$. This is acceptable agreement, considering the order of magnitude estimates of the various quantities involved. In

particular, the estimate of ρ in the region of the contact may be too low, owing to surface contamination and also to high stresses at the contact. In support of this, it has been observed that the resistance of Nb point contacts usually decreases by only a few percent between room temperature and the transition temperature, rather than by an order of magnitude or more as in pure bulk Nb. Assuming therefore a resistivity of $\sim 10^{-5} \Omega \text{ cm}$, instead of 10^{-6} , gives a contact radius $\sim 10^{-6} \text{ cm}$, in good agreement with value derived from the critical current. Yet another estimate of the contact area may be made from the load required to achieve contacts of the appropriate resistance and critical current. Taking an upper limit of yield strength $\sim 10^8 \text{ g/cm}^2$ and a load of 5 g gives an area $\sim 10^{-7} \text{ cm}^2$ or greater. This is several orders of magnitude greater than the previous estimates, and indicates quite definitely that an insulating surface film plays a mechanical role in supporting a very large part of the normal load on the contact. It is clear both from this and previous studies^{21,22} why the load is not in most cases a useful parameter to use in achieving the desired contact resistance and critical current.

Apparently then, the effective metal-to-metal contact area lies in the neighborhood of 10^{-12} cm^2 , for critical currents of the order of 10^{-6} A . The fact that suitable contacts are quite easy to make by the crude methods described in the preceding section seems a bit anomalous. There is in fact some experimental evidence that the true contact area is considerably larger than these calculations indicate. In the thin film experiments of Lambe *et al.*,¹⁰ interference effects were achieved rather consistently with necks a few microns wide in tin films about (presumably) 0.1μ thick. The apparent cross-sectional area was therefore of the order of 10^{-8} cm^2 . However, these experiments were carried out fairly close to the transition temperature so the critical current density might have been relatively low.

Meissner²³ has published the results of extensive measurements on superconducting contacts between bare tin wires and tin wires plated with various normal metals. Two points from his paper have been included in Fig. 12. Our work perhaps answers one question which was raised in connection with his work, namely, what is to be the criterion for superconductivity of such a contact? We suggest that the most rigorous criterion is the interference effect itself, and the implication of phase coherence through the contact. Also in Meissner's work it was shown that the load-bearing area of the contact is very much larger than the area calculated from the contact resistance, in agreement with our experience with untreated (i.e., off-the-shelf) wires.

We have seen that the normal-state resistance R of the point contact is typically of the order of 1 to 100Ω for critical currents in the milliampere-to-microampere

¹⁹ W. A. Little and R. D. Parks, *Phys. Rev. Letters* **9**, 9 (1962).

²⁰ L. Meyers and W. A. Little, *Phys. Rev. Letters* **11**, 156 (1963).

²¹ R. Holm, *Electric Contacts* (Springer-Verlag, Berlin, 1958).

²² M. Cocks, *Proc. Phys. Soc. (London)* **B67**, 238 (1954).

²³ H. Meissner, *Phys. Rev.* **109**, 686 (1958); **117**, 672 (1960).

range. This result is very similar to that obtained with Josephson junctions, for which an explicit microscopic theory has been developed. That this is no mere coincidence can be shown by the following qualitative arguments, still assuming the model of actual metal-to-metal contact. It has been shown²⁴⁻²⁶ that for thin films the current per unit length J has the form:

$$J = (ct/4\pi\lambda^2)A_s f(A - A_0/A_s),$$

where t is the thickness of the film, A the vector potential, λ the London penetration depth, and A_s a parameter of the material equal to $c\Delta/ev_F$ in the BCS theory. The function $f(x)$ has a maximum value close to unity. Therefore the maximum current at absolute zero for a film of width w is:

$$I_{\max} \cong \frac{c^2 tw}{4\pi\lambda^2} \frac{\Delta/e}{v_F} = \frac{a}{\rho l} \frac{\Delta}{e},$$

where l is the mean free path and $a = tw$ is the cross-sectional area. Now in the case of a narrow constriction in a thin film, or a small-area contact between two massive blocks of metal, it may happen that the transverse dimensions are comparable to or less than the bulk mean free path. Then the factor $a/\rho l$ in the above expression becomes of the order of l'/ρ , where l' is the transverse dimension, which is exactly the contact resistance R of a circular contact of diameter l' . It appears therefore that for our so-called point contacts the critical current should be of the order of the energy gap over the contact resistance, in rough agreement with experiment. This would not hold in general, as for example, for a thin-film device where the length of the constriction is much greater than its transverse dimensions. This may be one reason why the normal-state resistance is not a very good parameter to use in adjusting a point contact for a particular critical current.

Finally, we wish to make a few remarks as to how thermal noise limits the observability of the interference pattern. It has been pointed out that for a Josephson junction the binding energy $E = (\hbar/2e)I_c$, becomes of the order of room-temperature thermal energy for $I_c \sim 10^{-5}$ A. This has been used in interpreting the lack of experimental observation of the diffraction effects in junctions where I_c was less than a few microamperes. In the present work, however, we see the interference effect, with good signal-to-noise ratio, in systems where

$I_c \sim 10^{-7}$ A (see Fig. 8). Evidently in double-contact ring experiments such as ours there is a binding energy of the order of $\frac{1}{8}(\varphi_0^2/L)$ or less, corresponding to the energy difference between a maximum and a minimum of the interference pattern. For a case like that of Fig. 7, where $L \sim 10^{-8}$ H, the energy difference is $\sim 10^{-22}$ J, which is comparable to KT at 4.2 deg. The question then is, why are interference effects at these amplitudes easily observable while diffraction patterns in Josephson junctions are not, even with much larger critical currents? Possibly the answer lies in the use of rf filtering in the cryostat leads, a technique which was in fact suggested by Josephson himself.

IV. SUMMARY

- (1) We have shown long-range phase coherence, by means of the interference effect, in all superconductors tested. The periodicity-influx is always, within experimental error, $\hbar/2e$.
- (2) Peak-to-peak amplitude of the interference is not greater than φ_0/L . This in effect determines the signal-to-noise ratio and puts a practical limit on the enclosed area of the interference device.
- (3) There is no apparent limit on the perimeter around which interference may be demonstrated, provided the enclosed area is kept small.
- (4) Observations on the behavior of point contacts seem consistent with a model of direct metal-to-metal contact. However, it cannot be ruled out that surface contamination plays a role in some cases, particularly in view of the inconsistent data on hysteresis effects in the volt-ampere characteristic. The relationship between normal-state resistance and critical current for the point contact is shown to be in rough agreement with theory.
- (5) We have observed quantum interference with a period as small as 2×10^{-7} G with a measuring bandwidth of 10^8 cps. This was further instrumented to provide a direct reading galvanometer with a full scale sensitivity of 2×10^{-7} G, and demonstrates a range of device possibilities.

ACKNOWLEDGMENTS

The work reported here benefited greatly by its proximity to and the free exchange of information concerning the original work on macroscopic quantum interference using Josephson junctions and thin metal bridges in thin films. We are also pleased to acknowledge several useful discussions with A. Warnick concerning circuit applications, and the expert technical assistance of D. Radzwin.

²⁴ J. Bardeen, Rev. Mod. Phys. **34**, 667 (1962).

²⁵ R. H. Parmenter, RCA Rev. **26**, 323 (1962).

²⁶ P. Fulde and R. A. Ferrell, Phys. Rev. **132**, 2457 (1963).

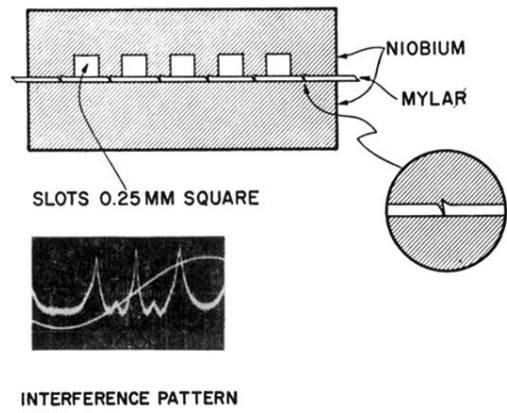


FIG. 10. Cross section of magnetic "diffraction grating" and interference pattern. Peak-to-peak field amplitude 1.8 mG.

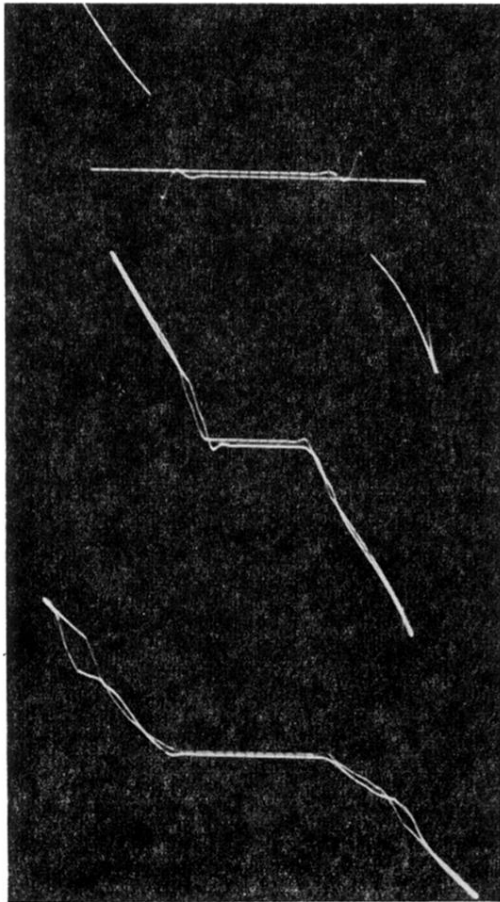


FIG. 11. "Typical" volt-ampere characteristics of point contacts.

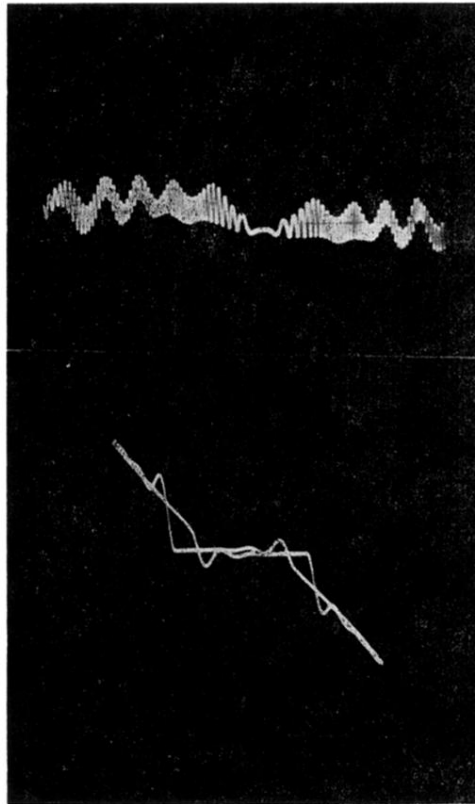


FIG. 5. Volt-ampere characteristic and interference pattern of crossed wires of Nb-Zr (15%) alloy.

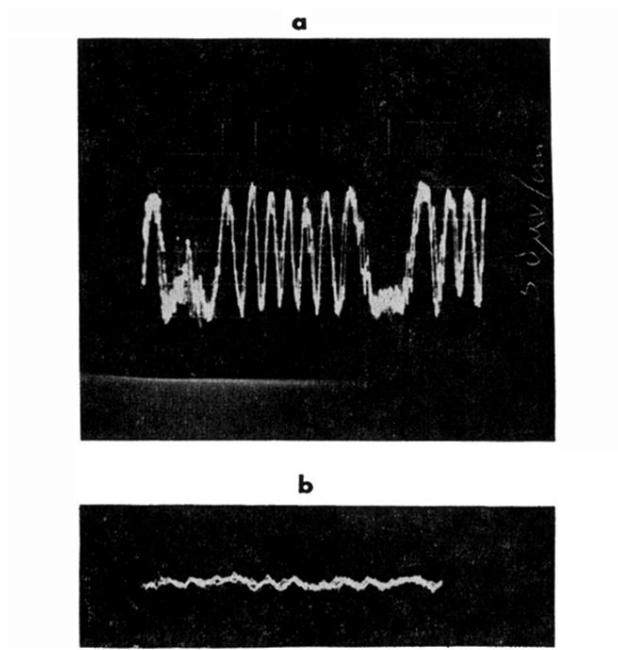


FIG. 8. Interference patterns of large-area devices in which noise is apparent. Both patterns are from devices like that shown in the lower part of Fig. 7. Dimensions: upper trace, $\frac{1}{4}$ in. i.d., $\frac{3}{4}$ in. o.d., $\frac{7}{8}$ in. long; lower trace, $\frac{3}{8}$ in. i.d., $\frac{3}{4}$ in. o.d., $\frac{7}{8}$ in. long. All leads into the cryostat were heavily filtered for frequencies above about 10^6 .

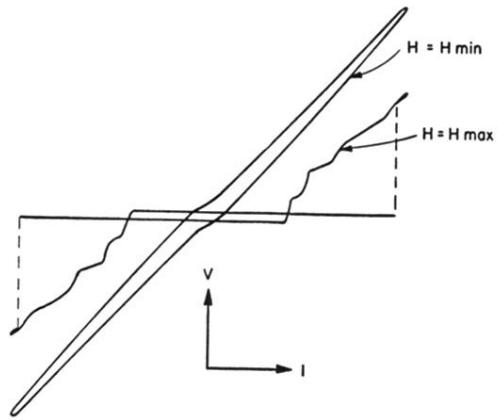
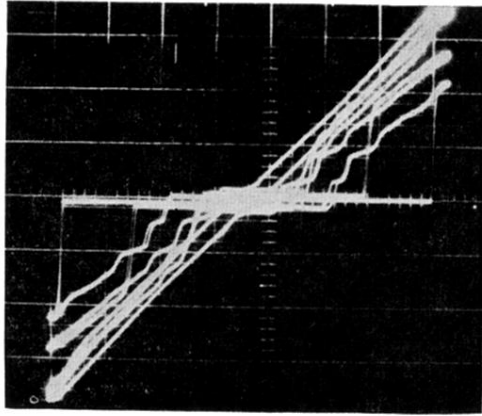


FIG. 9. Magnetic-field modulation of the volt-ampere characteristic for a (nontypical) case where I_e goes to zero periodically. The photograph is a superposition of traces for four different field values. The lower sketch is a tracing, for clarity of the two lines for which I_e is maximum and minimum, respectively.